Supplementary Information: Separating the Ferromagnetic and Glassy Behaviour Within the Metal-Organic Magnet $Ni(TCNQ)_2$

1 Structural Characterisation

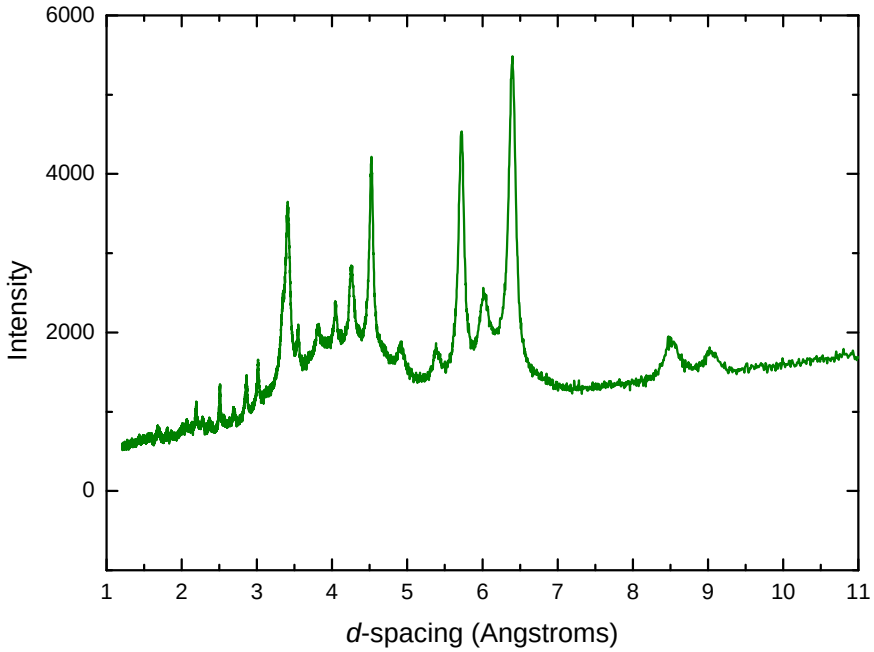

Figure 1: Powder X-ray diffraction data for $Ni(TCNQ\text{-}D_4)_2$ taken on a the I11 beam line at the Diamond Light Source.

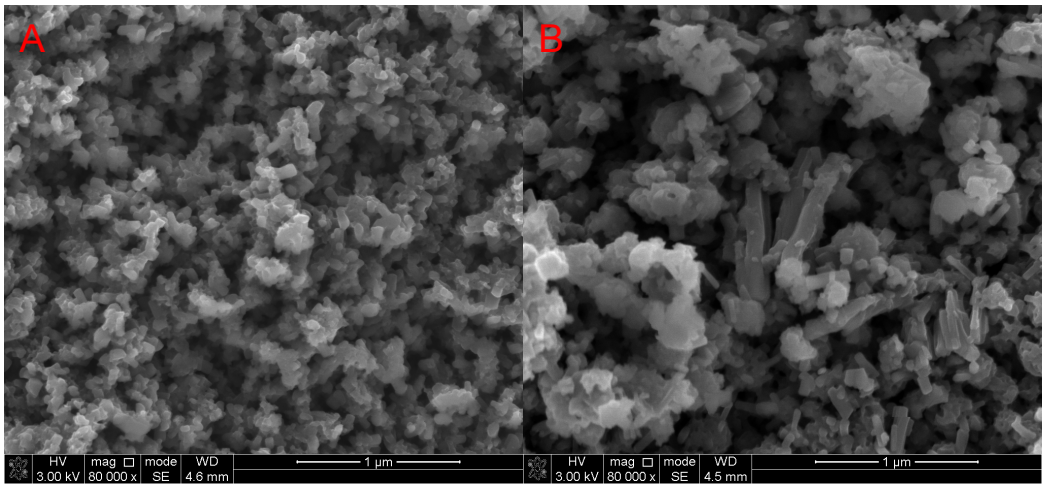

Figure 2: SEM images of both the protio (A) and deutero (B) forms of $Ni(TCNQ)_2$.

2 Magnetic Measurements

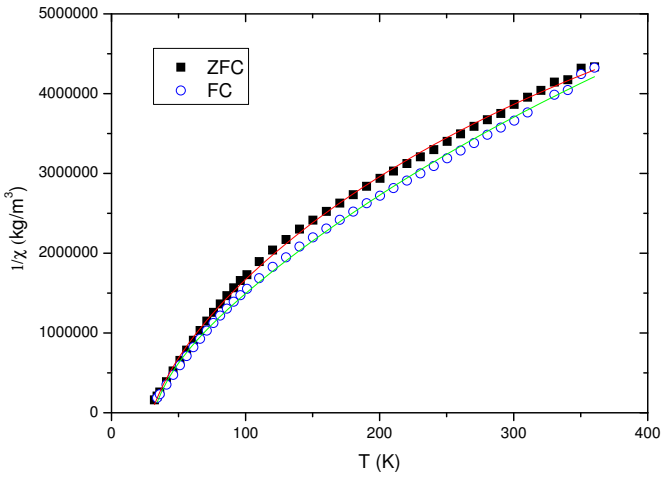

Figure 3: Inverse of magnetic susceptibility vs. temperature for $Ni(TCNQ\text{-}D_4)_2$. Filled squares: data obtained after zero field-cooling the sample; open circles: data obtained after field-cooling the sample in 2.5 mT. Solid Lines are fits to the data in the temperature range 34 K to 360 K using to equation 1. Fitting parameters are given in table 1.

The temperature dependence of the inverse susceptibility of $Ni(TCNQ\text{-}D_4)_2$ is shown in figure 3 for the range 34 K to 360 K; these data were obtained using a Quantum Design Magnetic Properties Measurement System. The data were taken in a field of 2.5 mT, with the field cooled (FC) results being obtained after cooling from 360 K to 2 K in 2.5 mT. Fits to both the zero field cooled (ZFC) and FC data were made using the equation [1],

$$\chi = \chi_0 + \frac{(C_A + C_B)T - 2(C_A C_B)^{0.5}\theta}{T^2 - \theta^2}, \tag{1}$$

which represents the sum of a ferrimagnetic response of the material and an additional temperature independent susceptibility (C_A and C_B are, respectively, the Curie constants for the A and B magnetic sublattices). The fit was performed using the variables χ_0, $A1 = C_A + C_B$,

$A2 = (C_A C_B)^{0.5}$ and θ. Values for the fitting parameters for both ZFC and FC results are given in table 1.

	χ_0 (m^3 kg^{-1})	A_1 (m^3 K kg^{-1})	A_2 (m^3 K kg^{-1})	θ (K)
ZFC	1.04(5) $\times 10^{-7}$	4.6(2) $\times 10^{-5}$	2(2) $\times 10^{-6}$	29.7(8)
FC	7.2(6) $\times 10^{-8}$	6.1(2) $\times 10^{-6}$	1.2(3) $\times 10^{-5}$	31(1)

Table 1: Parameters from a fit to the inverse susceptibility data in the temperature range of 34 K to 360 K.

It is noted that, for temperatures very close to θ, the ferrimagnetic form of the magnetic response approximates to a Curie-Weiss-like temperature dependence for the paramagnetic susceptibility with $\chi \sim (A1 - 2A2)/2(T - \theta)$. In this case one may expect the results shown in table 1 of the paper to be in agreement with the relevant fitting parameters shown in table 1. This seems to be the case for the θ values obtained from both fits, but the $(A1 - 2A2)/2$ values, while of the same order of magnitude, are smaller than Curie constant, C, given by the Curie-Weiss analysis. In fact the A_2 value obtained from the ZFC data is completely unreliable and suggests that equation 1 does not completely describe the temperature dependence of the susceptibility. Moreover, the parameter χ_0 is found to be positive for both the ZFC and FC fits which suggests that there are other contributions to the susceptibility that need to be accounted for in the fits to the data. Also, the data shown in figure 3 clearly demonstrate that there is a small component of the susceptibility that is sensitive to the field cooling of the sample; this remnant component appears to be thermally quenched at around about 350 K which rules out a magnetic contribution from bulk nickel.

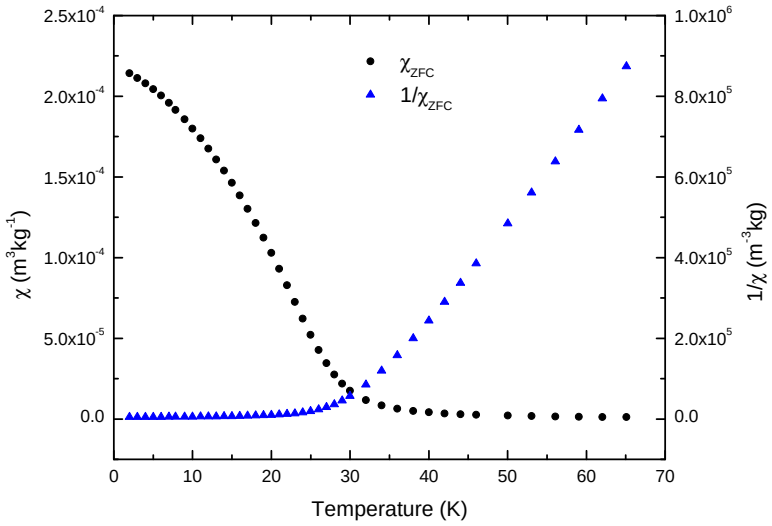

Figure 4: 0.1 T ZFC data for Ni(TCNQ-D_4)$_2$

Figure 4 shows a ZFC susceptibility within an applied field of 0.1 T where the hysteretic behaviour is suppressed. This data was used to show that at low temperatures the magnetization follows Bloch's law which is evidence for the 3D magnetic ground state.

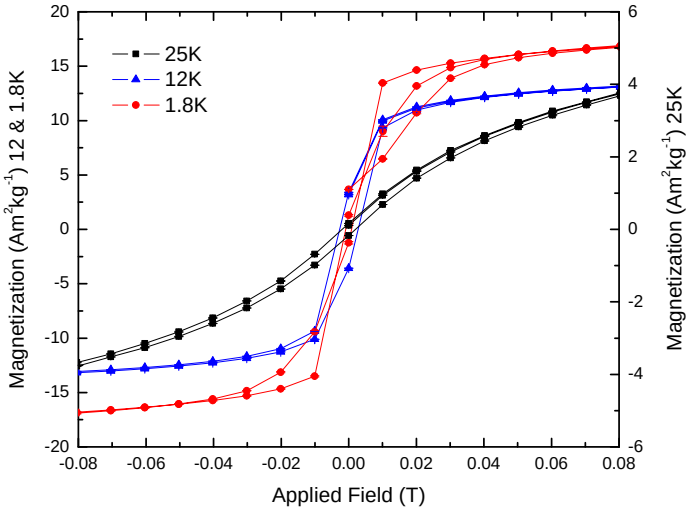

Figure 5: Low field magnetization vs. applied field data of figure 5 within the main text for showing the hysteresis present at all temperatures. Error bars are included however they are smaller than the data points.

3 Heat Capacity

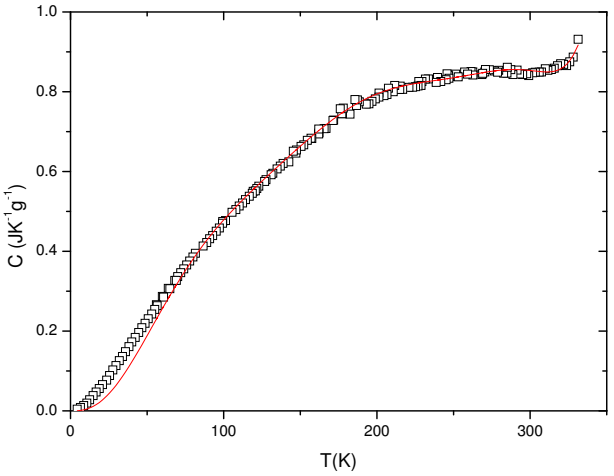

Figure 6: Heat capacity *vs.* temperature for Ni(TCNQ-D_4)$_2$. Solid Line is a fit to data in the temperature range 70 K to 340 K using to the function $C = \Sigma_n A_n T^n$ for $n = 3$ to 9.

The temperature dependence of the heat capacity is shown in figure 6 for the range 4 K to 340 K; these data were obtained using a Quantum Design Physical Properties Measurement System. Following a similar procedure to that outlined in reference [2], we fit the data between 70 K and 340 K using a polynomial function of temperature $C(T) = \Sigma_n A_n T^n$ where n varies from 3 to 9. The leading term $\propto T^3$ reflects the assumption that the the system behaves as a 3 dimensional solid. The value of 70 K was chosen to be a temperature which was sufficiently high so that magnetic contributions could be ruled out whilst low enough so that a significant T^3 was still present in $C(T)$; 70 K was also the lowest temperature at which there was an improvement in the fit to the heat capacity data with the the polynomial in T.

n	A_n (JK^{1-n}g^{-1})
3	4.9(1) $\times 10^{-6}$
4	-1.08(3) $\times 10^{-7}$
5	1.09(4) $\times 10^{-9}$
6	-6.0(3) $\times 10^{-12}$
7	1.88(9) $\times 10^{-14}$
8	-3.1(2) $\times 10^{-17}$
9	2.2(1) $\times 10^{-21}$

Table 2: Parameters from a fit to the experimental heat capacity data in the temperature range of 70 K to 350 K.

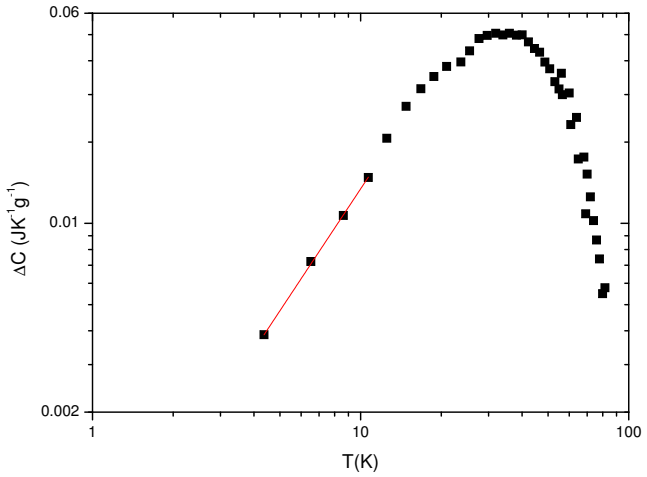

Figure 7: Difference in heat capacity vs. temperature for Ni(TCNQ-D_4)$_2$. Solid Line is a fit to the function $\Delta C = \alpha T^{3/2}$.

Figure 7 presents the difference between the measured heat capacity and that computed using the polynomial in T with the coefficients shown in table 2. The data are shown on a log-log scale and the linear variation of ΔC below about 10 K demonstrates that well defined power law. The solid red line is a fit to the low temperature data with a form $\Delta C = \alpha T^{1.5}$, the fitting parameter $\alpha = 4.24(2) \times 10^{-4}$ JK$^{-2.5}$g^{-1}.The value of α may be used with equation (15) to obtain a value of $J_{\rm ex}/k_B = 1.69(1)$ K when using the parameters listed in section B2. This value is about 15% larger than given in section B2, though is it is closer to the value obtained from the analysis of the low temperature $M(T)$ results described in section B1. Moreover, the temperature dependent magnetization data shown in figure 4 of the paper deviate from Bloch's law at above 10 K which is also the highest temperature for the fit to the form $\Delta C = \alpha T^{1.5}$ shown in figure 7 is applicable. Another feature in the data of figure 7 is a well defined step at about 24 K, which is approximately the value of temperature at which the steepest part of the M *vs.* T curve extrapolates to zero as shown in the inset of figure 4 of the paper. This suggests that there is evidence for the magnetic phase transition in the heat capacity data set and, though this is a small effect, it nevertheless tentatively supports the conclusion that properties of the ferromagnetic state of Ni(TCNQ-D_4)$_2$ can be detected in $C(T)$.

A final observation is that both the spin wave-like component of the heat capacity, and the small step at 24 K, are superimposed upon a broad heat capacity anomaly with a maximum at between 30 K and 40 K. This may indicate the presence of strong short-range order as ob-

served, for example, in the charge transfer complex decamethylferrocenium tetracyanoethenide [DMFc][TCNE] where 1D stacking of the TCNE anions occurs [3]. In the case of Ni(TCNQ-D_4)$_2$ it is possible that a quasi-one dimensional coupling of radical spins occurs along chains of stacked TCNQ-D_4 anions. Alternatively, the broad heat capacity anomaly may be a consequence of small magnetic clusters within the material[4].

References

[1] C. Kittel. Introduction to Solid State Physics 8th Edition. John Wiley and Sons, USA.

[2] M. Sorai, Y. Nakazawa, M. Nakano and Y. Miyazaki. *Chem. Rev.* **113** (2013) PR41-PR122

[3] M. Nakano and M. Sorai. *Chem. Phys. Lett.* **169** (1990) 27

[4] M. Nakano and M. Sorai. *Chem. Rev.* **113** (2013) PR41